JOURNAL OF MATERIALS SCIENCE 24 (1989) 963–973

Dynamic temperature crystallization behaviour of amorphous and liquid $Mg_{70}Zn_{30}$ alloy

Y. KHAN
Institut für Werkstoffe der Elektrotechnik, Ruhr Universität, D-4630 Bochum 1, West Germany

The crystallization behaviour of the amorphous and liquid $Mg_{70}Zn_{30}$ alloy was investigated using a dynamic temperature X-ray diffraction method (DTXD). The sequence of phases crystallizing from the amorphous state with increasing temperature was found to be the same as that of the phases crystallizing from the liquid state with decreasing temperature. At low heating rates (i.e. 20 K/h), it was found that the alloy $Mg_{70}Zn_{30}$ underwent a crystalline–amorphous transformation in the solid state, first at 440 K then at 590 K. This alloy showed the phenomenon of multimorphy; the different crystal structures form due to a macroscopic structural quantization effect. Structural data of new phases, discovered during this work, are given.

1. Introduction

Metallic glasses (i.e. amorphous metallic materials), are obtained mostly by rapid quenching from the liquid state and hence must retain some characteristics reminiscent of the high-temperature state [1]. Dynamic temperature X-ray diffraction (DTXD) analysis (i.e. X-ray diffraction analysis during continuously changing temperature [2]) of the metallic glasses reveals that the reminiscence is always the primary phase that crystallizes first from the amorphous state [3, 4]. DTXD investigations have been limited to a study of crystallization from amorphous state. It would be of great interest to extend this method to study crystallization behaviour of easy glass-forming liquids. In the present work, the results of the DTXD analyses of amorphous and liquid Mg–Zn alloys, with compositions close to the glass-forming alloy $Mg_{70}Zn_{30}$, are reported.

The Mg–Zn system was chosen because of low melting temperatures of the alloys in this system and hence it could be investigated conveniently in our DTXD apparatus. Although crystallization behaviour of the Mg–Zn amorphous alloys has been investigated by Altounian *et al.* [5] by the DSC method, a DTXD investigation of these amorphous alloys, with which crystal structures are brought directly to observation during a crystallization process [2], has not been carried out.

2. Experimental details

Mg–Zn alloys (weighing about 200 g), with composition close to $Mg_{70}Zn_{30}$, were prepared by melting the alloy constituents under argon gas in a Balzers medium frequency induction furnace, using MgO crucibles. The melts were cast into a water-cooled copper mould. The purity of the elements 99 995 wt % for both Mg and Zn. The Mg–Zn metallic glasses were prepared in the form of thin ribbons (3 mm wide, 30 to 40 μm thick, 10 to 15 m long) by spinning the alloy melt on a copper roller. Chemical analysis was carried out by atomic absorption spectroscopy with an accuracy of better than 1 wt %.

For the DTXD analysis, a modified Guinier–Lenne high-temperature X-ray camera was used [2]. The X-ray source was a Co-anode Philips fine focus X-ray tube with a power rating of 1200 W. The DTXD patterns of Mg–Zn metallic glasses and melts during crystallization were taken for different heating rates and crystallization times. The X-ray exit slit was 5 mm in width. The film speed was 5 mm/h throughout this work. For room temperature X-ray diffraction, an Enraf–Nonius Guinier camera was used. The microdensitometer analysis (MDA) (i.e. the evaluation of the intensities and Bragg angles of the X-ray reflections), was carried out by using a modified Zeiss–Jena MD-100 instrument. Differential thermal analysis was carried out in Al_2O_3 sample holders, using a Linseis DTA apparatus. For heating rates 1200 K/h (Fig. 6), a specially constructed thermal analysis apparatus was used.

3. Results and discussion

The thermal structural behaviour of the amorphous $Mg_{70}Zn_{30}$ alloy during and after crystallization was found to be complex, in agreement with the findings of Altounian *et al.* [5]. Fig. 1 shows dynamic temperature X-ray diffraction patterns of a liquid-quenched amorphous (LQA) $Mg_{70}Zn_{30}$ alloy taken in the temperature range from 300 to 600 K and back at a heating and cooling rate, respectively, of 20 K/h. These heating and cooling rates are so low that one can assume quasi-isothermal conditions during heat treatment of the alloy.

3.1. Amorphous state of $Mg_{70}Zn_{30}$

In the X-ray diffraction pattern of the LQA $Mg_{70}Zn_{30}$

0022–2461/89 $03.00 + .12

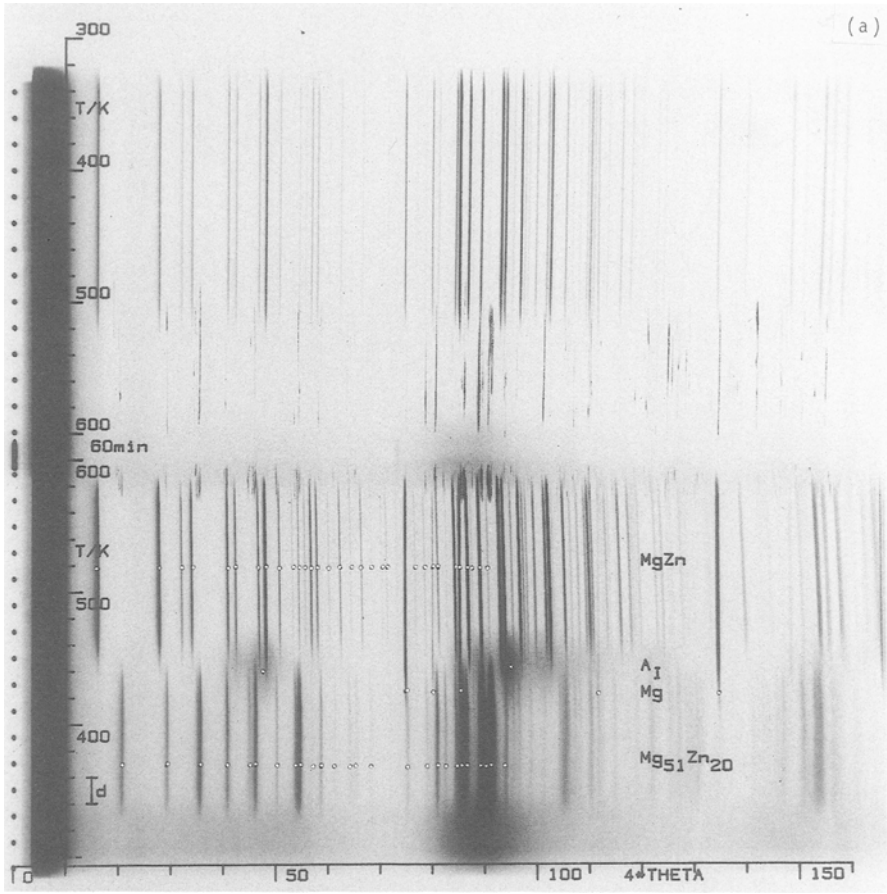

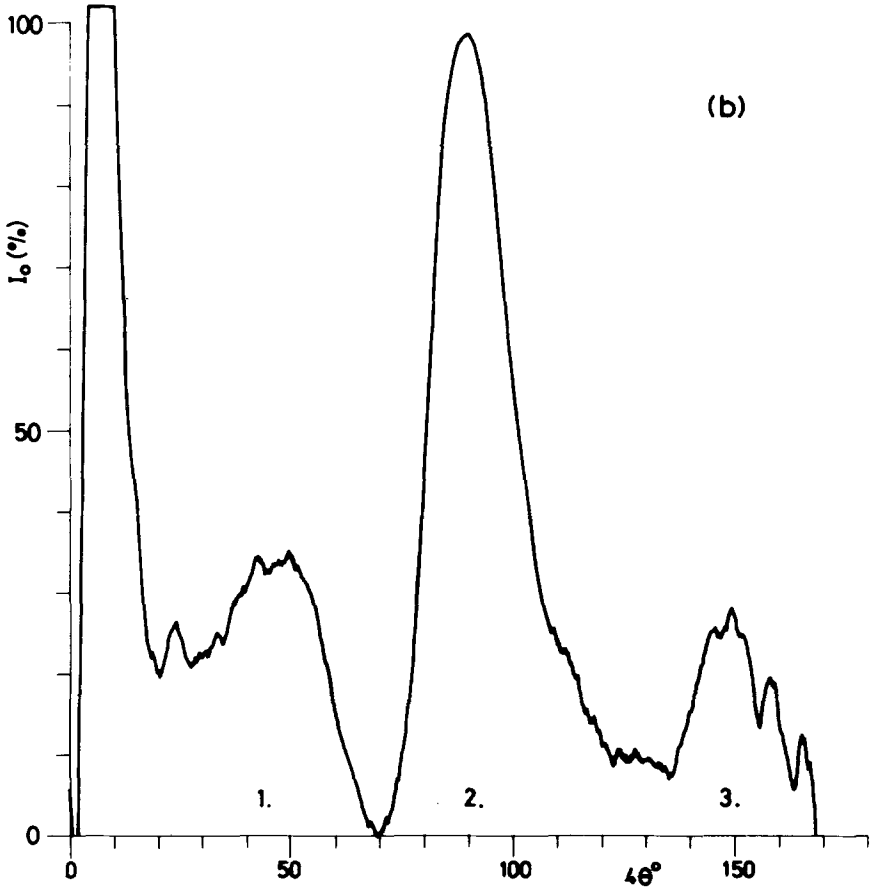

Figure 1 (a) DTXD pattern of the LQA $Mg_{70}Zn_{30}$ alloy taken in the temperature range 300 to 600 K with a temperature hold for 1 h at 600 K. The X-ray exit slit width is given by *d*. The reflections marked with empty dots on a horizontal line belong to the phase printed on the right. A_i stands for the intermediate amorphous state. The black dots along the ordinate mark the position of the direct beam. Along the ordinate these dots can be used to calibrate the temperature/time axis. For the abscissa these points can be used to measure the Bragg angle 4θ; (b) MDA scan at 310 K; (c) at 530 K on the heating path; (d) at 400 K on the cooling path of (a).

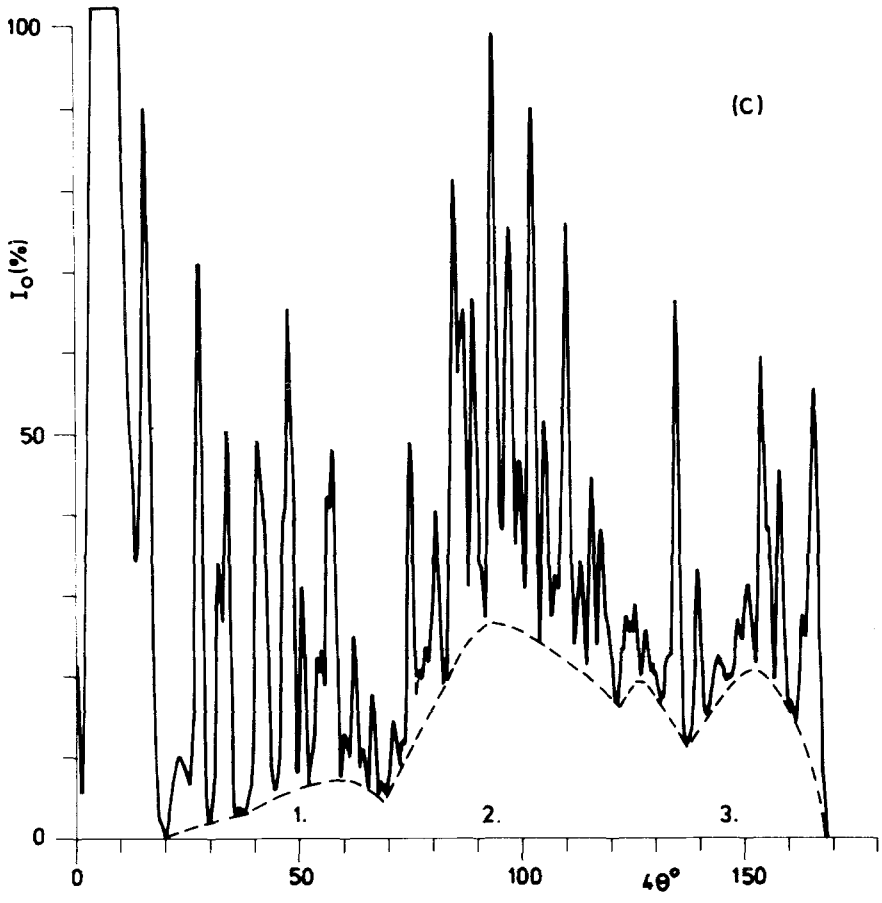

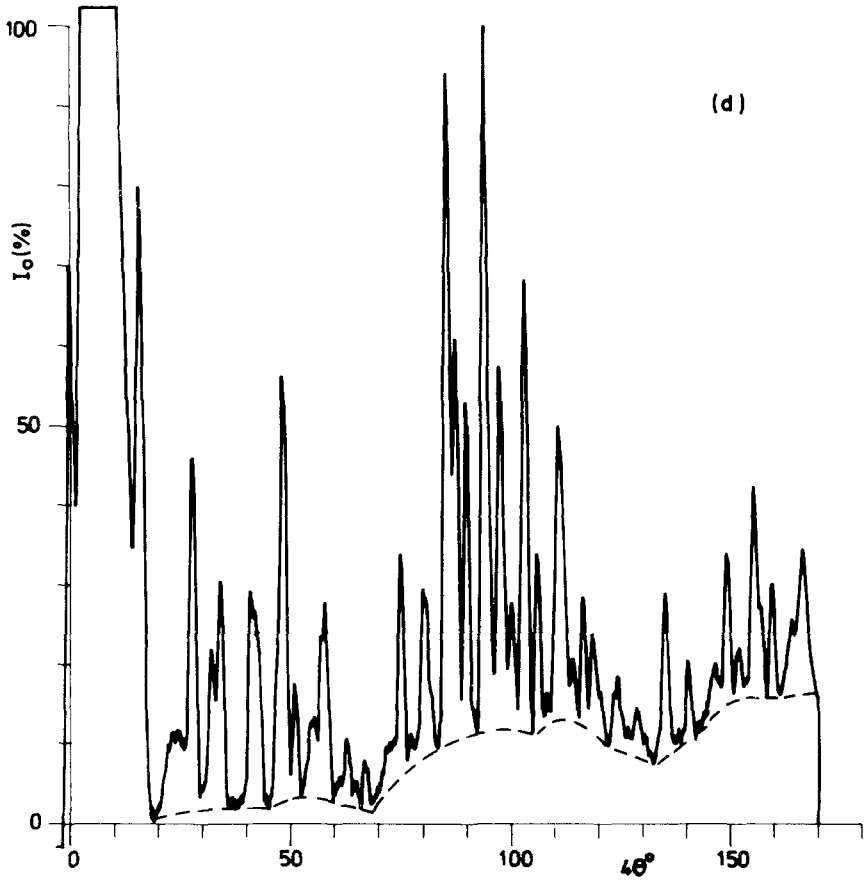

Figure 1 Continued

alloy, three diffraction halos with centres at diffraction angles $4\theta = 46°$, 88.5° and 147° in the intensity sequence, weak, strong, weak, could be observed (cf. Figs 1a and b). In general, an amorphous material gives rise to Fraunhofer-type diffraction halos, however, in the intensity sequence of strong, weak, very weak, due to lack of periodicity [6]. Scrutiny of the observed halos reveals that the second halo is not homogeneous and symmetrical as regards the distribution of its intensity; the halo is strong in the range $81° < 4\theta < 92°$ and seems to fade away steadily from $4\theta > 92°$ to $4\theta < 120°$ (Fig. 1b). This halo may be due to two types of non-crystalline material, one giving rise to the halo part in the range $81° < 4\theta < 92°$ (left side) and the other giving rise to the halo part in the range $92° < 4\theta < 96°$ (right side). The halo in the range $96 < 4\theta < 120$ is structured; the origin of this halo part is not clear. A simple calculation shows that the halos at $4\theta = 46°, 94° = (92° + 96°)/2, 147°$ are 1st, 2nd and 3rd order reflections, respectively, from an elementary unit of diffraction with a period of 0.529_8 nm (Table I). Since the lattice parameter, a, of the $MgZn_2$-structure is 0.528_8 nm and lattice parameters of the other structures in the Mg–Zn system are simply multiples of this unit, these three halos seem to be due to microcrystalline regions of the $MgZn_2$-type which could have been formed on rapid cooling. The intense part of the middle halo occurs almost in the same 4θ-range in which the halos due to the amorphous Fe–B [3], Co–B [7] and Cu–Zr [8] alloys have been reported and may be due to a real amorphous state.

There is a controversy on the amorphous state of matter. The older view is that the amorphous materials are made up of very tiny microcrystals [9]. This "microcrystal" model is, however, shadowed by the works of Warren [10], Scott [11] and Bernal [12], who believe that the structure of an amorphous solid is liquid-like or Bernal-type (i.e. the atoms are randomly densely packed in the amorphous solid). There are some experimental results, regarding e.g. to X-ray diffraction, volume contraction at the amorphous crystalline temperature, the dependence of the specific heat on temperature, which favour the Bernal-type model. There are, however, experimental results regarding e.g. cooperative phenomena such as ferromagnetism, electrical conductivity and elastic properties, which suggest that the structure of an amorphous solid must be of the microcrystalline-type, thus preserving the necessary short-range order.

From our experimental results on the amorphous $Mg_{70}Zn_{30}$ alloy, we conclude that the amorphous state is of dual nature (i.e. there was amorphous solids whose structure is of the microcrystalline-type and solids whose structure may be of the Bernal-type). An amorphous solid may be a mixture of both. The change of state from amorphous to crystalline and vice versa is continuous (i.e. the crystalline phase grows continuously from the amorphous material and the amorphous state emerges continuously from the crystalline state. The nature of the amorphous state depends only upon the matter-type, preparation conditions and stability against whole-scale crystallization.

3.2. Crystallization from the amorphous state of $Mg_{70}Zn_{30}$

At the heating rate 20 K/h, a part of the LQA $Mg_{70}Zn_{30}$ alloy appeared to crystallize at about 340 K, because it was at this temperature that the diffraction halos disappear and X-ray reflections, characteristic of a periodic structure, appeared (Fig. 1). These reflections could be indexed on the basis of an orthorhombic unit cell of the $Mg_{51}Zn_{20}$-type [13] with lattice parameters, $a = 1.425_3$ nm, $b = 1.455_1$ nm and $c = 1.415_3$ nm. As is seen, these reflections were diffuse and broad, implying that either the crystallized material was extremely fine (causing line broadening due to crystallite size) or made of isomorphous phases of varying lattice parameters (i.e. parametric line broadening). It was difficult to decide what contributed to the line broadening in this case. It may have been due to both.

At ca. 345 K, recrystallization of $Mg_{51}Zn_{20}$ took place, as seen by the appearance of the diffraction lines due to hexagonal Mg (Fig. 1). The phase, $Mg_{51}Zn_{20}$, was not stable and decomposed at ca. 450 K into Mg and an equilibrium phase. The structures of the Mg–Zn intermediate phases other than Mg_2Zn_{11} [14], $MgZn_2$ [14] and $Mg_{51}Zn_{20}$ [13] are not known yet. Although the formation of the phases, MgZn and Mg_2Zn_3, has been reported [15], their structural data are not available in the literature. We believe that the equilibrium phase forming after decomposition of $Mg_{51}Zn_{20}$ is the phase MgZn. The X-ray diffraction lines due to this phase could be indexed on the basis of a rhombohedral unit cell (for $-h + k + l = 3n$) with lattice parameters, $a = 2.56_9$ nm, $c = 1.810_4$ nm (Table II).

MDA of the DTXD pattern of the LQA $Mg_{70}Zn_{30}$ alloy revealed that a certain amount of the amorphous material remained uncrystallized even up to the melting temperature of that material. We demonstrated

TABLE I X-ray diffraction data for the amorphous $Mg_{70}Zn_{30}$ alloy

Temperature (K)	Halo positions								d* (nm)
	1		2				3		
			Left side		Right side				
	$\sin^2\theta_0$	$\sin^2\theta_c$	$\sin^2\theta_0$	$\sin^2\theta_c$	$\sin^2\theta_0$	$\sin^2\theta_c$	$\sin^2\theta_0$	$\sin^2\theta_c$	
~310	0.0397	0.0398	–	–	0.1590	0.1590	0.3580	0.3578	0.530
	–	–	0.1491	0.1491	–	–	–	–	0.273_5
~540	0.0402	0.0400	–	–	0.1598	0.1600	–	–	0.526_7

*d value was calculated by the formula given by Guinier [6] with $k = 1.18$

TABLE II Structural data of the phase MgZn

hkl	$\sin^2\theta_0$	$\sin^2\theta_c$	I_0 (%)
101	0.0048	0.0041	90
110		0.0049	
300	0.0146	0.0147	70
220	0.0195	0.0197	35
122	0.0218	0.0212	50
003		0.0220	
312	0.0315	0.0310	50
321	0.0339	0.0336	40
140		0.0344	
232	0.0412	0.0408	40
051	0.0435	0.0434	65
330		0.0442	
241	0.0486	0.0483	30
511	0.0532	0.0532	15
422	0.0558	0.0556	20
413		0.0562	
600	0.0582	0.0585	20
134	0.0607	0.0601	40
152		0.0605	
015	0.0628	0.0622	45
431		0.0630	
205	0.0678	0.0676	10
161	0.0728	0.0729	25
440	0.0774	0.0780	10
351	0.0825	0.0821	15
701			
235	0.0921	0.0920	10
116		0.0929	
262	0.0943	0.0949	10
360	0.1033	0.1024	50 (Mg)
164	0.1092	0.1092	15
452		0.1096	
802	0.1140	0.1145	20
704	0.1177	0.1190	20 (Mg)
354			
345	0.1213	0.1212	40
146		0.1216	
615	0.1307	0.1310	80
900	0.1327	0.1327	60
280	0.1382	0.1376	65
544		0.1386	
137	0.1405	0.1400	10
535		0.1408	
075			
407	0.1456	0.1449	70
265		0.1457	
327	0.1502	0.1498	30
526		0.1511	
814	0.1579	0.1583	100
562		0.1587	
057	0.1600	0.1597	100

this effect on the formation of the equilibrium phase, MgZn. This phase formed on heating the LQA $Mg_{70}Zn_{30}$ alloy above 450 K and on cooling the melted $Mg_{70}Zn_{30}$ alloy below 500 K. The MDA scans taken at 530 K on the heating and at 400 K on the cooling path of Fig. 1a are given in Figs 1c and d, respectively. As is seen, the background level (given by dashed lines) is much greater when the MgZn phase forms after crystallization from the amorphous state (Fig. 1c) than when the MgZn phase forms after crystallization from the liquid state (Fig. 1d). Since the shape of this background level is similar to the shape of the curve due to amorphous state (Fig. 1b), it is concluded that a part (estimated to be ca. 20%) of the amorphous material remains uncrystallized up to 530 K, a temperature close to the solidus (595 K). A systematic study of MDA of DTXD of the LQA $Mg_{70}Zn_{30}$ alloy showed that 30 to 40% of the amorphous material remained uncrystallized at the regular crystallization temperature. The amount of this residual amorphous material decreased with increasing temperature until the material melted. It appears as if the reminiscent state acquired by the alloy during rapid quenching is so stable that this can only be destroyed after remelting. The reminiscent stability of the amorphous state up to the solidus may explain the discrepancy between the heat of crystallization from the liquid and amorphous states i.e. the heat of crystallization of an amorphous alloy amounts only to ca. 25 to 50% of the heat of crystallization from the liquid state [8].

3.3. An intermediate unstable amorphous phase

Before the equilibrium phases Mg and MgZn were formed by decomposition of $Mg_{51}Zn_{20}$, an intermediate metastable amorphous phase came into existence as seen by the appearance of diffraction halos with centres at $4\theta = 46.3°$, $94.3°$ and intensity sequence of medium, strong, respectively (Figs. 1, 2, 4 and 5, and Table I). The diffraction angles of this amorphous phase were found to be somewhat larger than those of the amorphous $Mg_{70}Zn_{30}$ alloy. This state could only be reached by heating to about 440 K a rapidly quenched crystalline or amorphous bulk or ribbon form $Mg_{100-x}Zn_x$ alloy for $x < 35$. If, during the DTXD experiment, the temperature were held constant close to the temperature of this decomposition while the film is still moving, details of the decomposition mechanism of the material in this unstable state were revealed (Fig. 2). This formed at ca. 430 K and decomposed partially into Mg and MgZn as is seen by the appearance of X-ray reflections due to both these phases after an annealing time of 1.5 h at ca. 440 K. At the same time, the diffraction halos disappeared into bands of diffuse reflections. These reflections could be indexed on the basis of a hexagonal unit cell of the $MgZn_2$-type with lattice parameters, $a = 0.528_8$ nm, $c = 0.870_4$ nm.

The isothermal heat-treatment experiments in the temperature range 420 to 480 K with the rapidly quenched bulk $Mg_{70}Zn_{30}$ alloys revealed that the phase $MgZn_2$ formed in the temperature range 435 to 460 K by decomposition of the $Mg_{51}Zn_{20}$ phase and existed when quenched from a temperature within this temperature range for weeks together, without further decomposition. However, this phase was unstable and transformed back to $Mg_{51}Zn_{20}$ simply by mechanical treatment (e.g. mechanical grinding).

The splitting of the X-ray diffraction reflections due to Mg and MgZn in the DTXD pattern during and

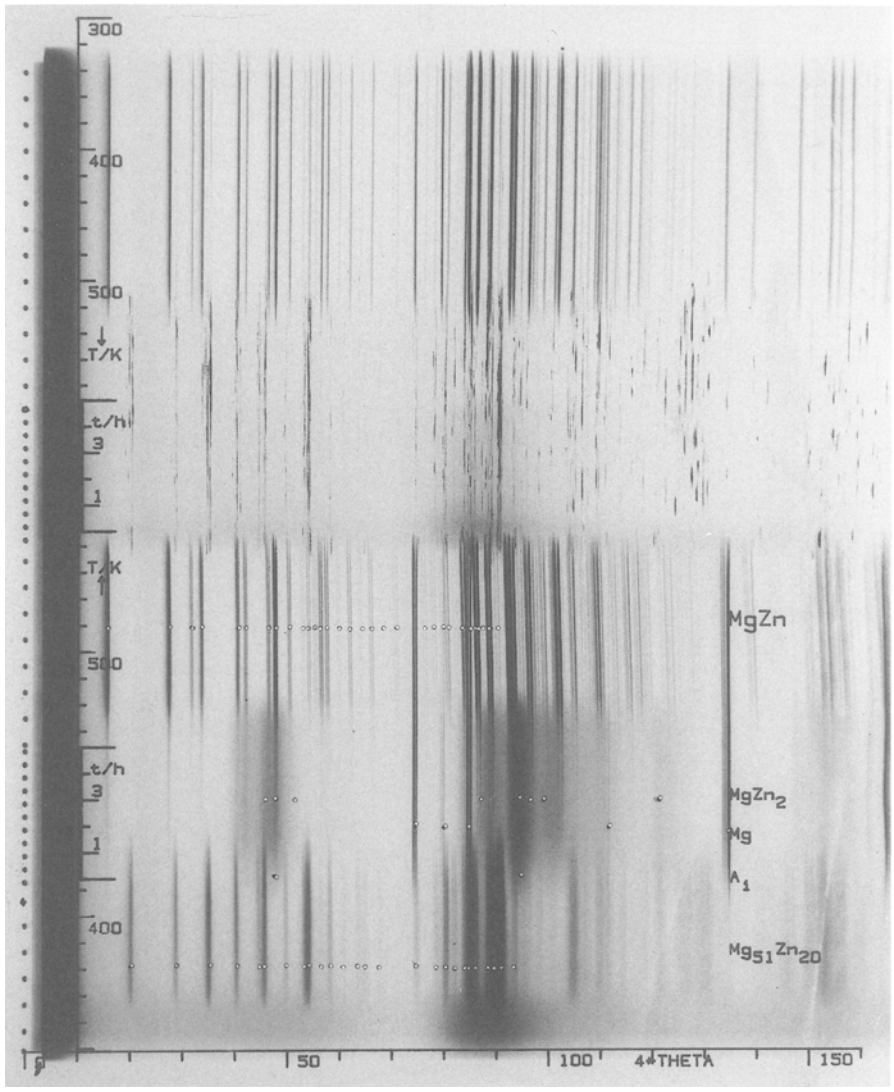

Figure 2 DTXD pattern of the LQA $Mg_{70}Zn_{30}$ alloy taken in the temperature range 300 to 590 K with temperature holds for 5 h at 430 and 590 K, respectively. Other details are the same as Fig. 1.

after isothermal annealing at 440 K for 5 h (Fig. 2) was noteworthy and might be due to an incoherent parametric change in the material as a result of a spinodal type decomposition of $Mg_{51}Zn_{20}$ because this was absent in the same DTXD pattern on the cooling path. As seen, all the reflections were doublets. Since this line splitting was also almost absent in the other DTXD patterns (cf. Figs 1a, 3–5), the line splitting seemed to be inherent to the isothermal heat treatment used in taking the DTXD pattern of Fig. 2.

3.4. Macroscopic quantization effect

On further heating the $Mg_{70}Zn_{30}$ alloy, the phases, Mg and MgZn, reacted to form the primary phase, $Mg_{51}Zn_{20}$, at ca. 580 K as revealed by the DTXD pattern. It is seen that the highest temperature phase was the same which crystallized first from the amorphous state in accordance with findings in the Fe–B system [3, 4]. However, the X-ray reflections were now split into extremely fine, sharp reflection lines (Figs 1 and 2). A similar observation has already been made by the author in the Co-rich Co-B alloy [1]. A detailed investigation of the instrumental set-up revealed that this line splitting was real and characteristic of the alloys which easily become amorphous on liquid quenching. In order to demonstrate this effect, we took a DTXD pattern of $Mg_{70}Zn_{30}$ (which can be easily melt-quenched in the amorphous state and remains in the amorphous state for years, cf. Fig. 3a) and a DTXD pattern of $Mg_{80}Zn_{20}$ (it is very difficult to melt-quench this alloy in the amorphous state and if quenched in the amorphous state, crystallizes partially at room temperature in a short time, cf. Fig. 3b). Before cooling down to room temperature, the temperature was held for 10 h at ca. 590 K. In the case of $Mg_{80}Zn_{20}$ (Fig. 3b), there was no line splitting of the reflections due to $Mg_{51}Zn_{20}$. However, in the case of $Mg_{70}Zn_{30}$ (Fig. 3b), the splitting of the reflections due to $Mg_{51}Zn_{20}$ was so large that it was difficult to index all of the diffraction lines. Had the splitting in Fig. 3a been due to occasional formation of large crystals (as a result of a camera artifact), the X-ray reflections in Fig. 3b would have been broad for the same reason. That this was not the case can easily be seen from Fig. 3b. The intermittency of the diffraction reflections along the time/temperature axis is noteworthy and may be due to a high gradient of chemical activity in the sample. It should be mentioned that this chemical activity must be absent in the case of the $Mg_{80}Zn_{20}$ alloy or at least must be so low that it was not seen in 10 h at 590 K.

The line splitting of the reflections due to $Mg_{51}Zn_{20}$ could only be due to parametric change (i.e. the $Mg_{51}Zn_{20}$ structure must have a high solubility for both Mg and Zn), given by a formula of the type $Mg_{1+y}Zn_{2-y}$ as will be discussed later.

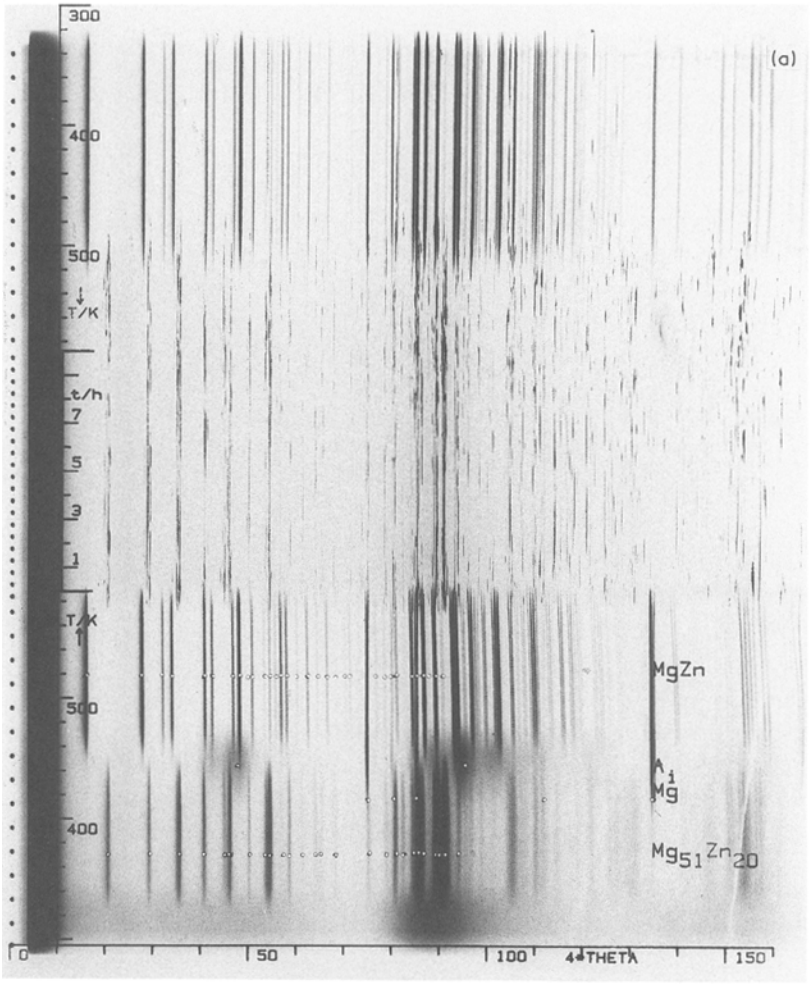

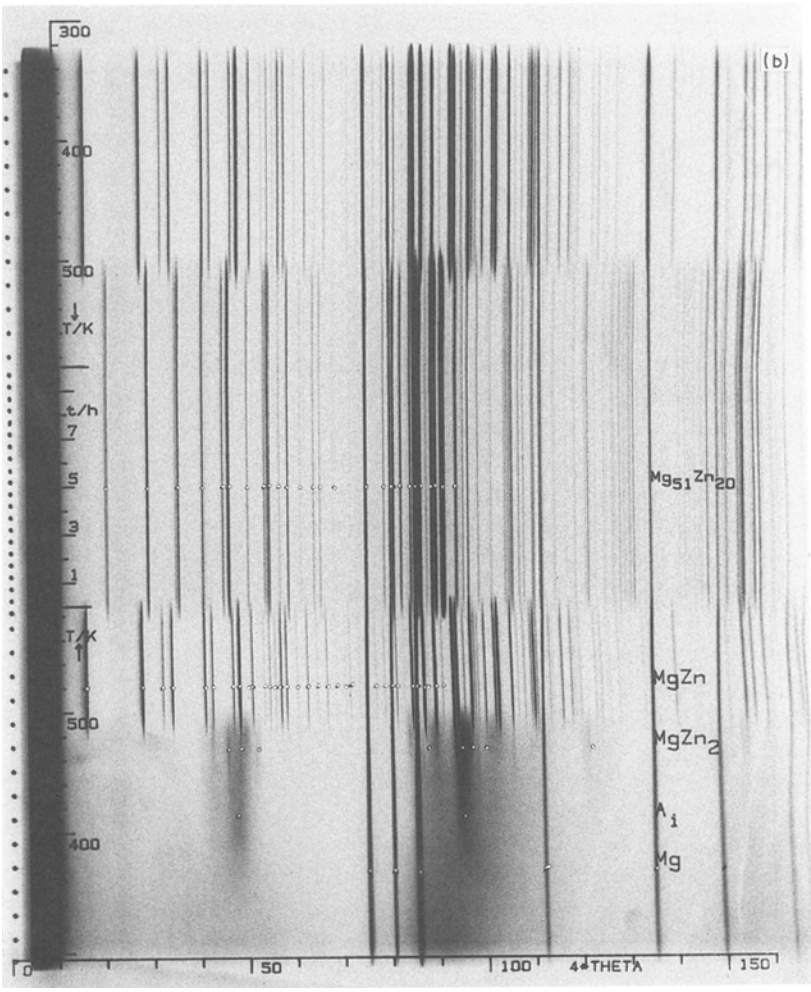

Figure 3 DTXD pattern of the LQA (a) $Mg_{70}Zn_{30}$, (b) $Mg_{80}Zn_{20}$ alloys taken in the temperature range 300 to 590 K with a temperature hold for 10 h at 590 K. Other details are the same as Fig. 1.

Due to the gradient of the chemical activity, caused by the solubility of Mg and Zn in $Mg_{51}Zn_{20}$, close to its decomposition temperature, structure dispersion (i.e. formation of coherent crystal structures with slightly different lattice parameters of a fundamental structural unit) may take place, such that the lattice parameters did not remain the same throughout the material. Since the splitting of the diffraction lines was very sharp, it was concluded that the crystal structures were discrete and hence the parametric change in the material occurred in steps of a fundamental unit or was discrete, quantized in a similar way as has been reported for the rare-earth–cobalt systems [16]. Had the parametric change been continuous, broad and diffuse diffraction reflections would have been observed.

3.5. Amorphization of $Mg_{70}Zn_{30}$ close to solidus

If the temperature were increased to ca. 590 K, the X-ray reflections disappeared and amorphous diffraction halos appeared at ca. the same positions at which diffraction halos due to the LQA $Mg_{70}Zn_{30}$ alloy were observed (Figs 1 and 2). It appeared that the sample melted, but the sample did not show any sign of this. On further heating to ca. 595 K, these diffraction halos disappeared and a diffraction halo characteristic of liquids appeared in the range $81° < 4\theta < 92°$ (Figs 1 and 2). It was about at this temperature that the sample showed a small sign of melting, as observed under a light-microscope.

The formation of an amorphous-like material close to solidus at so low heating rates as 20 K/h is very surprising and suggests that the amorphous state belongs to the phase diagram close to the solidus at least in the Mg–Zn system within a certain concentration range. By rapid quenching, the high-temperature amorphous state of the alloy has simply frozen-in. This leads to the conclusion that at least the Mg–Zn amorphous alloys are not undercooled liquids as has been universally assumed for metallic glasses. This result is in agreement with the findings of the author in the binary Co–B [1] system and the quasi-binary Fe_3B–Ni_3B system [17] that in these systems amorphous alloys were formed only if the melts did not undercool, suggesting that the amorphous alloys on the basis of Fe–B, Co–B, Fe–Ni–B and Mg–Zn might not be undercooled liquids.

3.6. Melting of the $Mg_{70}Zn_{30}$ alloy

The melting of the $Mg_{70}Zn_{30}$ alloy was not sharp, contrary to what would be expected for a metallic material. The melting process in this alloy had been found to depend upon the heating rate (Fig. 6). At the heating rate used in DTXD work (20 K/h), the melting began at 595 K (i.e. the solid alloy began to soften at this temperature) and extended to ca. 615 K (i.e. the melting range was ca. 20 K). At the heating rate of 300 K/h (usually used in DTA), the melting was found to begin at 618 K and to end at ca. 660 K (i.e. the melting range extended over a temperature range of ca. 42 K (Fig. 6). In this sense, the melting behaviour of the $Mg_{70}Zn_{30}$ alloy resembles the melting characteristic of a non-metallic glass in which the range of melting is much larger (e.g. it is ca. 700 K for SiO_2).

3.7. Crystallization from the liquid state of $Mg_{70}Zn_{30}$

The crystallization on cooling, from the liquid state of $Mg_{70}Zn_{30}$ was found to depend sensitively upon the absolute temperature of the melt and the time for which the melt was kept at that temperature. If $Mg_{70}Zn_{30}$ was heated to 600 K and after 1 h at that temperature, cooled down, the phase $Mg_{51}Zn_{20}$ formed without any undercooling (Fig. 1). As is seen, this phase then existed up to 500 K, after which it decomposed into the Mg and MgZn phases. It is noteworthy that the X-ray diffraction lines due to $Mg_{51}Zn_{20}$ were split and intermittent. The line splitting could only be due to parameteric changes in the material as a result of concentration gradients. If this effect had been due to formation of large crystals, the diffraction lines would have fallen almost on the same position due to the focussing nature of the DTXT camera [2]. Such a crystallization behaviour is typical for metastable super-saturated solid solutions (i.e. it may be that on cooling, a metastable supersaturated solid solution of the $Mg_{51}Zn_{20}$-type enriched in Zn or of the $MgZn_2$-type enriched in Mg forms. If the decomposition of such a solid solution proceeded through discrete coherent isomorphous phases, a number of diffraction lines corresponding to the same hkl triple would result. A detailed study of this effect will be presented elsewhere.

If the alloy was heated to ca. 605 K and then cooled down, a new yet unkown phase crystallized first instead of $Mg_{51}Zn_{20}$. The undercooling is found to be ca. 10 K (Fig. 4). However, if the alloy was heated to ca. 610 K and then cooled down, a second unknown phase formed (Fig. 5). The undercooling was found to be not > 10 K in this case.

These two new phases existed up to room temperature, if kept free of mechanical shocks. On mechanical treatment (e.g. grinding, hammering) both these phases were found to transform into the $Mg_{51}Zn_{20}$ phase. The X-ray reflections due to both these new phases could be indexed on the basis of tetragonal unit cell with $a = 2.027_8$ nm and $c = 1.064_9$ nm.

It follows that crystallization from the melt of the $Mg_{70}Zn_{30}$ alloy is a very complicated process. The temperature of the melt and the time, for which the melt was kept at that temperature, determined the structure of the phase crystallizing from the melt. The $Mg_{70}Zn_{30}$ melt was capable of crystallizing in a large number of crystal modifications, many of which were metastable and might decompose during rapid quenching, due to their mechanical sensitivity. It should be mentioned that the $Mg_{70}Zn_{30}$ melt was found to be so highly viscous that the metallic alloy ribbons could support themselves freely in the DTXD-chamber at 610 K for 1 h.

3.8. The phase diagram and phase relations

The crystal structures of the different phases in the Mg–Zn system are closely related and the lattice parameters of these phases are related with one another as

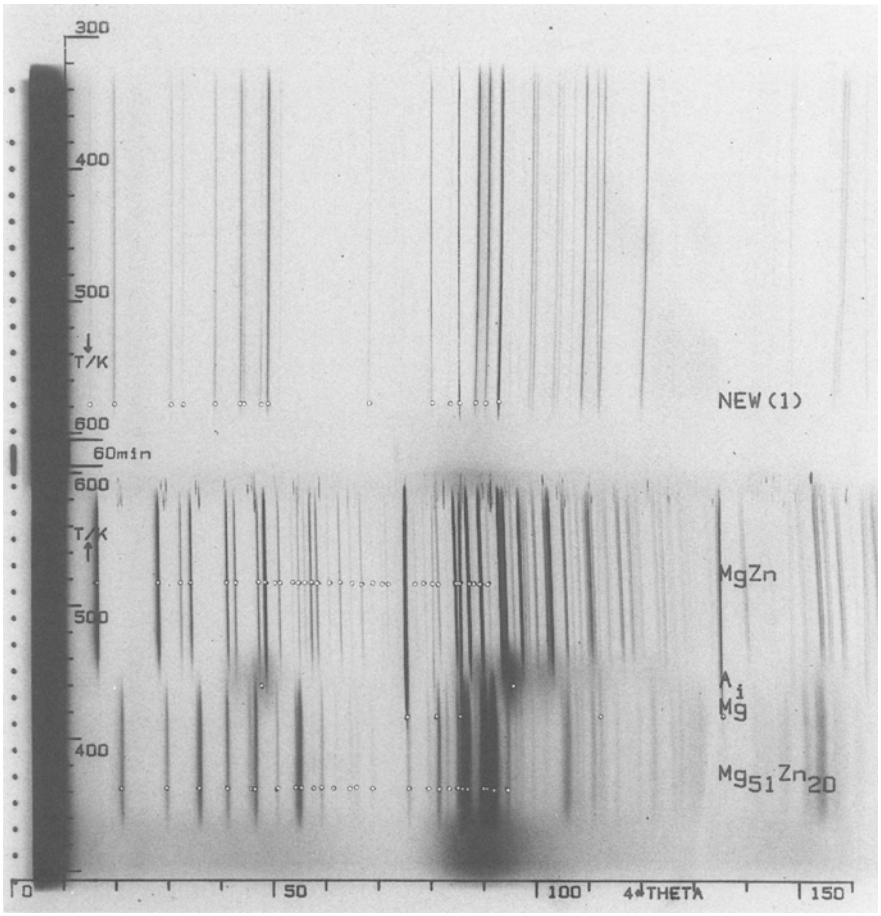

Figure 4 DTXD pattern of the LQA $Mg_{70}Zn_{30}$ alloy taken in the temperature range 300 to 605 K with a temperature hold for 1 h at 605 K. Other details are the same as Fig. 1.

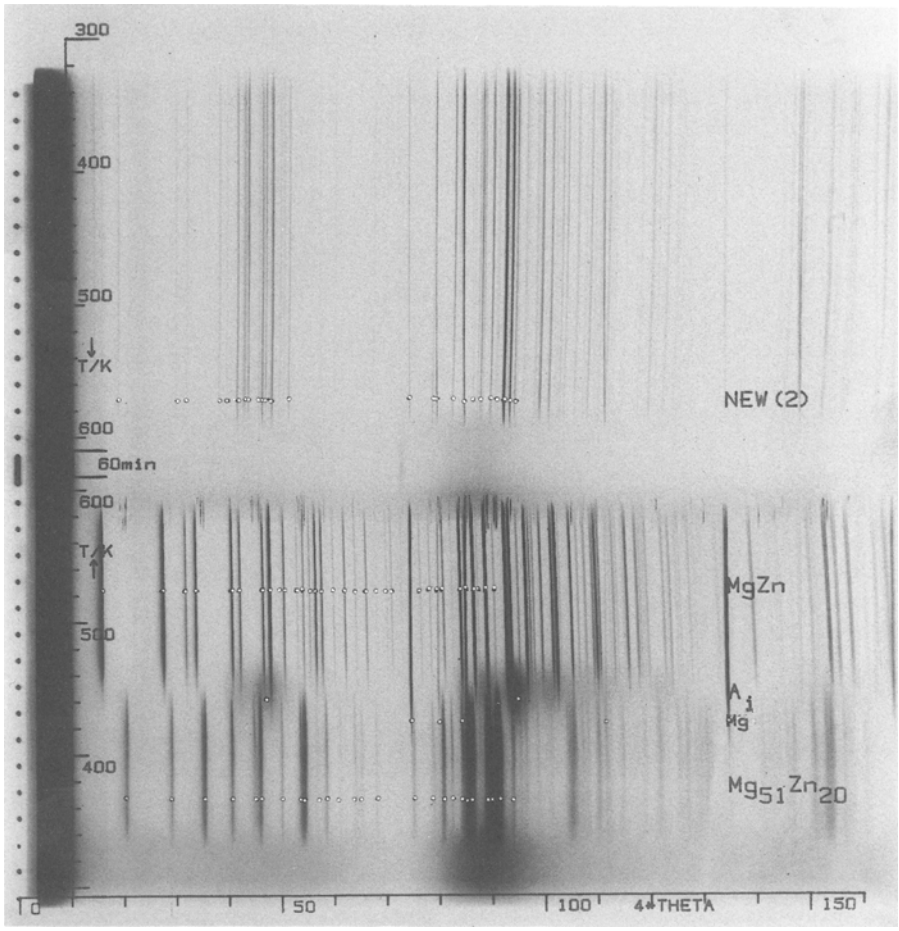

Figure 5 DTXD pattern of the LQA $Mg_{70}Zn_{30}$ alloy taken in the temperature range 300 to 610 K with a temperature hold for 1 h at 610 K. Other details are the same as Fig. 1.

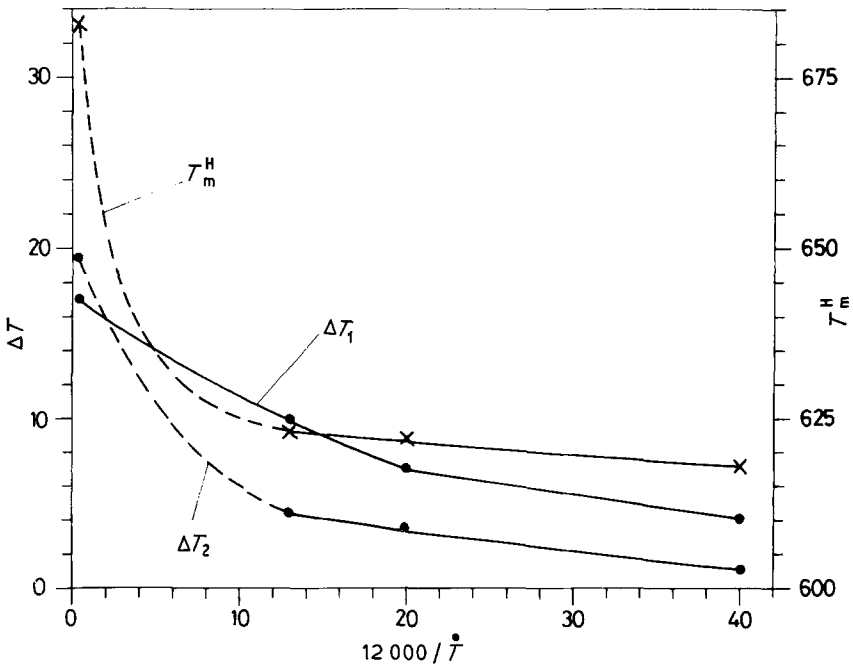

Figure 6 Dependence of the melting temperature of $Mg_{70}Zn_{30}$ on the heating rate. T_m^H = temperature at the beginning of melting on heating: T_s^K = temperature at the beginning of solidification on cooling: T_m^{H0} = temperature of melting (612 K) on heating at the rate 60 K/h. $\Delta T_1 = T_m^{H0} - T_s^K = \Delta T$; $\Delta T_2 = T_m^H - T_s^K = 5 \times \Delta T$, in order to use the same scale for $\Delta T_1 = f(T)$ and $\Delta T_2 = f(T)$. (x) $T_m^H K$; (●) $\Delta T K$; ($\dot{T}$) K/h.

follows:

$$a_{Mg_{51}Zn_{20}} = 2\sqrt{2} \times a_{MgZn_2},$$
$$b_{Mg_{51}Zn_{20}} = \sqrt{3} \times c_{MgZn_2},$$
$$c_{Mg_{51}Zn_{20}} = a_{Mg_{51}Zn_{20}},$$
$$a_{MgZn} = 5 \times a_{MgZn_2},$$
$$c_{MgZn} = 1.5\sqrt{2} \times c_{MgZn_2},$$
$$a_{\text{new phase}} = 4 \times a_{MgZn_2},$$
$$c_{\text{new pahse}} = 2 \times a_{MgZn_2}.$$

It is seen that the lattice parameters of all of the higher Mg–Zn phases can be derived from those of the $MgZn_2$ phase by simple relations. Through substitutions (Mg for Zn and vice versa), or atomic displacements, or both, one phase may transform into the other. On the basis of the above results and of DTXD investigations, we constructed a hypothetical phase diagram for the Mg–Zn system as given in Fig. 7, showing the phenomenon of multimorphy. Note that the phase MgZn forms peritectoidally and not peritectically. The two phase region, Mg + $MgZn_2$,

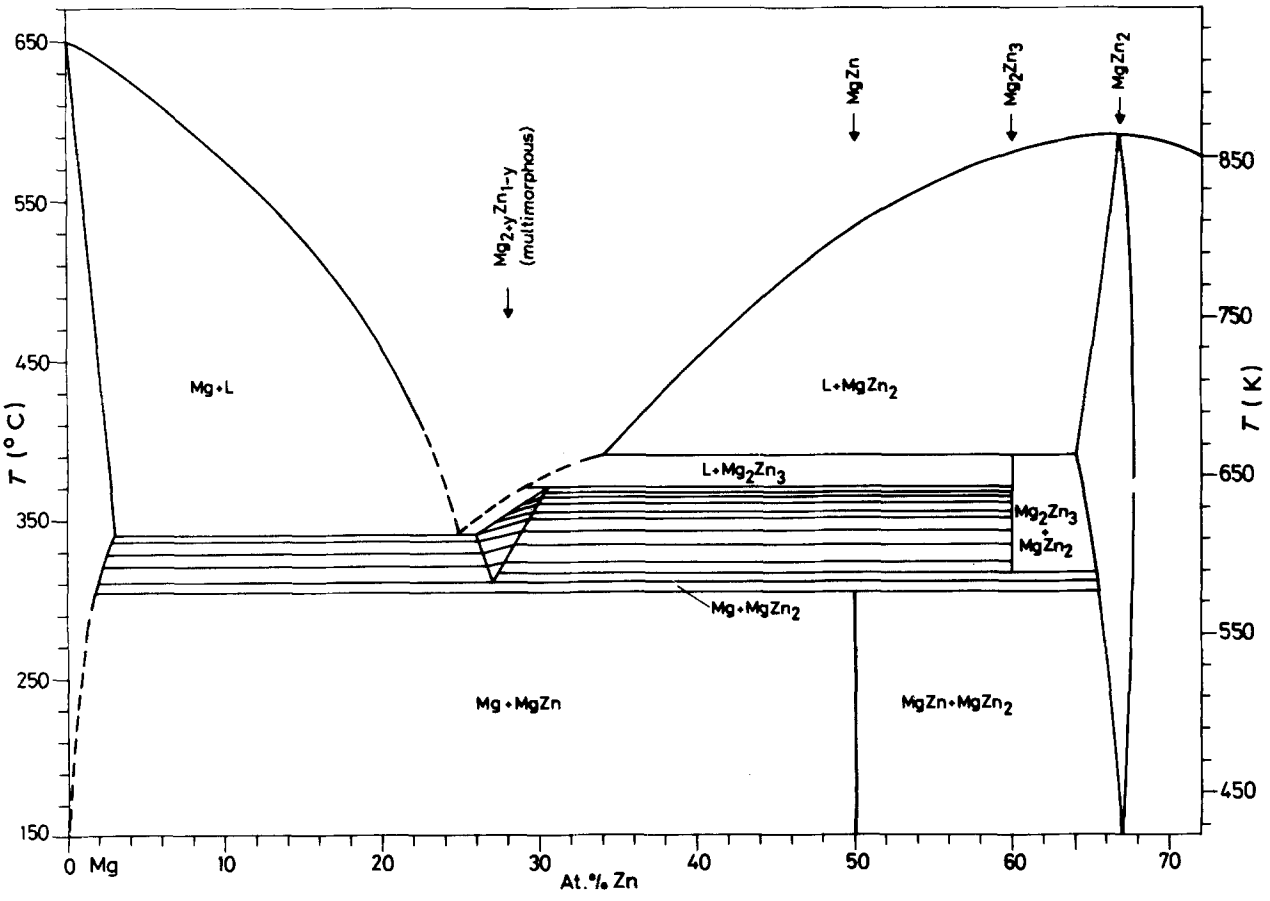

Figure 7 A section of the equilibrium phase diagram of the Mg–Zn system, showing the phenomenon of multimorphy.

existed only in a very small temperature range. In our opinion, it is this phase region which was responsible for the amorphization of the phase $Mg_{51}Zn_{20}$ in the solid state (cf. Fig. 1).

It should be noted that during and after crystallization from the amorphous state, a reversal of the equilibrium phase diagram seemed to take place with increasing temperature (i.e. the sequence of phases crystallizing from the amorphous state with increasing temperature was the same as the sequence of phases crystallizing from the liquid state with decreasing temperature). This was in agreement with the findings of the author in the Co–B system [1] and Fe–B system [3, 4].

3.9. Glass formation mechanism

If the $Mg_{70}Zn_{30}$ melt was rapidly quenched, some metastable or unstable phases formed and decomposed under the mechanical shock to which the samples were rendered during rapid quenching. Through this decomposition new metastable and/or unstable phases might form. The decomposition and phase formation reactions continued until the melt solidified. In view of this, the amorphous $Mg_{70}Zn_{30}$ material would consist of a large number of slightly varying unit cells. In our opinion, these cells were the $MgZn_2$-type and had a distorted lattice, otherwise we would get the X-ray patterns of an isostructural solid solution. A study of the structures found in the $Mg_{70}Zn_{30}$ alloys close to the solidus revealed that the structure of this alloy possessed two degrees of freedom (i.e. at constant concentration, the $Mg_{70}Zn_{30}$ phase existed in a number of modifications as a function of temperature and at constant temperature, this phase existed in a number of modifications having isomorphous structures as a function of concentration. In the former case, this is described as polymorphy. However, in the latter case, no terminology is yet known. Since, in this case, a concentration change plays an important role, we may call it merimorphy (Gr. meria = side). Both polymorphy and merimorphy can be termed as multimorphy (Fig. 7). The multimorphy in the alloys close to the composition $Mg_{70}Zn_{30}$ can be designated by the formula $Mg_{1+y}Zn_{2-y}$, the value of y depending upon the position of the alloy in the phase diagram. The phase $Mg_{51}Zn_{20}$ should then be a limiting member of the structural family on the Mg-rich side. Since the detailed structures of the members of this family were not known, the exact correlation between the different structures in the Mg–Zn system could not be postulated. The temperature spacing in the multimorphous phases appeared to decrease with increasing temperature, (i.e. the density of phases per temperature interval increased with increasing temperature (Fig. 7)). For the sake of simplicity, only a limited number of phase modifications of $Mg_{70}Zn_{30}$ are shown in Fig. 7. In a similar way, it would be expected that the density of phases per concentration interval increased with decreasing value of y. Obviously, the greater the phase density, the greater the phase dispersion. We therefore state that the phenomenon of multimorphy is essential for the formation of glasses. Detailed investigations are still being carried out.

Acknowledgement

The financial support of the Deutsche Forschungsgeminschaft (DFG) for this project is gratefully acknowledged.

References

1. Y. KHAN, *J. Non-Crystalline Solids* **86** (1986) 137.
2. *Idem. J. Phys. E: Sci. Instru.* **85** (1985) 1054.
3. Y. KHAN, E. KNELLER and M. SOSTARICH, *Z. Metallkde.* **72** (1981) 563.
4. E. KNELLER, Y. KHAN, V. GEISS and J. VOßKÄMPER, *ibid.* **75** (1984) 698.
5. Z. ALTOUNIAN, T. GUO-HUA and J. O. STROMOLSEN, *J. Mater. Sci* **17** (1982) 3268.
6. A. GUINIER, "X-ray Diffraction" (Freeman, San Francisco, 1963) p. 73.
7. Y. KHAN, T. ABBAS and S. A. SHAHEEN, *J. Mater. Sci. Lett.* **3** (1984) 319.
8. E. KNELLER, Y. KHAN and U. GORRES, *Z. Metallkde.* **77** (1986) 152.
9. J. T. RANDALL, H. P. ROOKSBY and B. S. COOPER, *J. Soc. Glass Technol.* **14** (1930) 219.
10. B. E. WARREN, *J. Appl. Phys.* **8** (1937) 645.
11. G. D. SCOTT, *Nature* **188** (1960) 908.
12. J. D. BERNAL, *Proc. Roy. Soc.* **A284** (1964) 299.
13. I. HAGASHI, N. SHIOTANI, M. UDA, T. MIZOGUCHI and H. KATOH, *J. Solid State Chem.* **36** (1981) 225.
14. K. SCHUBERT, "Kristallstrukturen zweikomponentiger Phasen" (Springer, Heidelberg, 1964) pp. 161, 221.
15. J. B. CLARK and F. N. RHINES, *Trans AIME* (1957) 425.
16. Y. KHAN, *Acta Cryst. B* **30** (1974) 1533.
17. Y. KHAN and V. GEISS, *Z. Metallkde.* **74** (1983) 317.

Received 16 November 1987
and accepted 24 May 1988